

Induced Seismicity Around Masjed Soleyman Dam, South West of Iran



M.Ebrahimi & M.Tatar

International Institute of Earthquake Engineering and Seismology, Tehran

SUMMARY:

During impounding of the Masjed Soleyman reservoir regards to national and international catalogues such as International Institute of Earthquake Engineering and Seismology (IIEES) and EHB catalog, an increase in seismic rate have been observed in the dam region, and 90 days after completing the impounding, an earthquake with moment magnitude of $M_w=5.6$ was occurred in the close vicinity of Masjed Soleyman reservoir. We installed a local seismic network of 5 seismological stations in the area since June 2006 for 15 months. The largest recorded earthquakes during the monitoring of Masjed Soleyman reservoir have magnitudes of $M_L=3.9$ and $M_L=3.6$. Statistical methods such as study of water level changes with variation of regional seismicity, foreshocks and aftershocks pattern, and correlation between the fractal dimension and the b-value used to identifying induced earthquakes occurred in the dam region.

Keywords: Masjed Soleyman dam, Induced seismicity, fractal dimension, b-value

1. introduction

Reservoir-induced Seismicity (RIS) is the triggering of earthquakes by physical processes that accompany the impoundment of large reservoirs. Impoundment of a reservoir and changes in lake levels can induce seismicity in two ways (Roeloffs 1988; Simpson et al. 1988). First, the rapid response due to elastic stress changes and second, the delayed response as a result of diffusion of pore pressure. The filling of large reservoirs modifies the tectonic stress regime, either by increasing the vertical stress through the effect of loading or by increasing the pore pressure, which results in a decrease in the effective normal stress. The net effect on existing fault zones is to increase or decrease stresses depending on the orientation and the geometry of the reservoir and the fault system (Snow 1972; Gupta and Rastogi 1976; Roeloffs 1988; Mekkawi et al. 2004).

Masjed Soleiman dam is located in 25.5 kilometer north-east of Masjed Soleiman city, Khuzestan Province, Southwestern Iran (see Fig. 2.1). Power generation, irrigation and flood control benefits will also be available as a result of the project installations.

Masjed Soleiman is a Rockfill dam with vertical clay core enjoying 177 m height from the foundation. The crest length is 497 m, and the width on the foundation is 15 m. The volume of the reservoir at normal level of 372m is 261 million cubic meters, and the length of the lake at normal level is 27 km. The dam was constructed between 1991 and 2000, and filling started on December, 2000.

The local seismographic network for Masjed Soleyman dam was established in June 2006, four years after filling the dam. This network recorded numerous weak events in a period of 15 months, indicating a considerable increase in the occurrence of earthquakes.

The objective of this article is identifying the induced earthquakes in the area and separating them from tectonic ones by using some methods such as: studying the water level changes with seismicity of the area, foreshocks and aftershocks patterns and estimating the fractal dimension.

2 Data

In the mid-2006, a digital seismograph network of five medium-band stations consist of Trillium-40T , 40 sec - 50 Hz seismometer connected to 24 bit Nonometric Taurus recorder was established around

the axis and reservoir of the Masjed Soleyman dam site by International Institute of Earthquake Engineering and Seismology (IIEES)(see Fig. 2.1).

The earthquake catalog of Masjed Soleyman network since June 1, 2006 to October 1, 2007 contains 3609 events. As the epicenter of induced earthquakes are mostly within the 30 kilometers radius of dam and their hypocenter is located at depth less than 10 kilometers (Gupta et al. 1972), therefore we selected out only 1924 events (Fig. 2.1) which satisfied above selection criteria. In the monitoring period of site the two large earthquakes with magnitude of 3.9 and 3.6 struck the area on November 23, 2006 and September 1, 2007, respectively. These earthquakes happened following a rapid change in water level of the dam (see Fig. 2.1 & table 3.2).

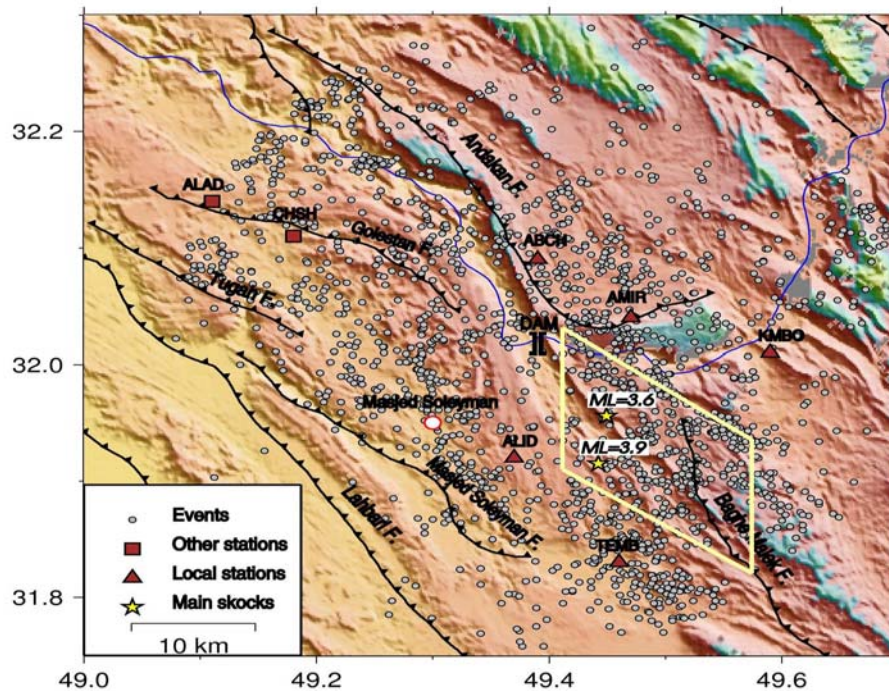


Figure 2.1. Earthquakes in Masjed Soleyman dam region in 30 km radius from dam site and 10 km depth.

3 METHODOLOGIES

More than one year of seismic events recorded by Masjed Soleyman seismological network in addition of 7 other permanent stations of Gotvand-e-Olya and INSN seismological network were analyzed by using an appropriate velocity model (Table 1) which calculated from 1-D inversion of arrived times, we relocated all recorded earthquakes.

Table 3.1. 1-D velocity model of region

Layer Number	Thickness (km)	P wave speed (km)	Vp/Vs ratio
1	0	5.2	1.85
2	11	6.0	1.85

3.1. Water Level Changes and Seismicity

Induced seismicity depends on the absolute water level to the extent that virtually all of the major bursts of seismicity occur when the water level is near or above any previous maximum (Gupta et al. 1972).

Since there were no local seismographic networks in the vicinity of Masjed Soleyman dam site, before and after the filling, seismic information in that time is limited. In spite of this fact, by having the water level changes since the beginning of filling, we tried to use recorded earthquakes in national and international stations such as International Institute of Earthquake Engineering and Seismology

(IIEES) catalog and corrected ISC (EHB, Engdal et al. 2006) catalog, to study the relation between water level changes and occurrence of earthquakes.

Table 3.2. Two main shocks during a 15-month period monitoring of the Masjed Soleyman dam site

Date	Longitude (degree)	Latitude (degree)	Magnitude (M_L)	Depth (m)
23/11/2006	49.509	31.905	3.9	9.2
01/08/2007	49.478	31.944	3.6	9.7

Fig. 3.1 shows the monthly number of earthquakes in the Masjed Soleyman dam site (30 kilometers radius from dam) in EHB and IIEES catalogs and water level changes since starting the impoundment in December 12, 2000.

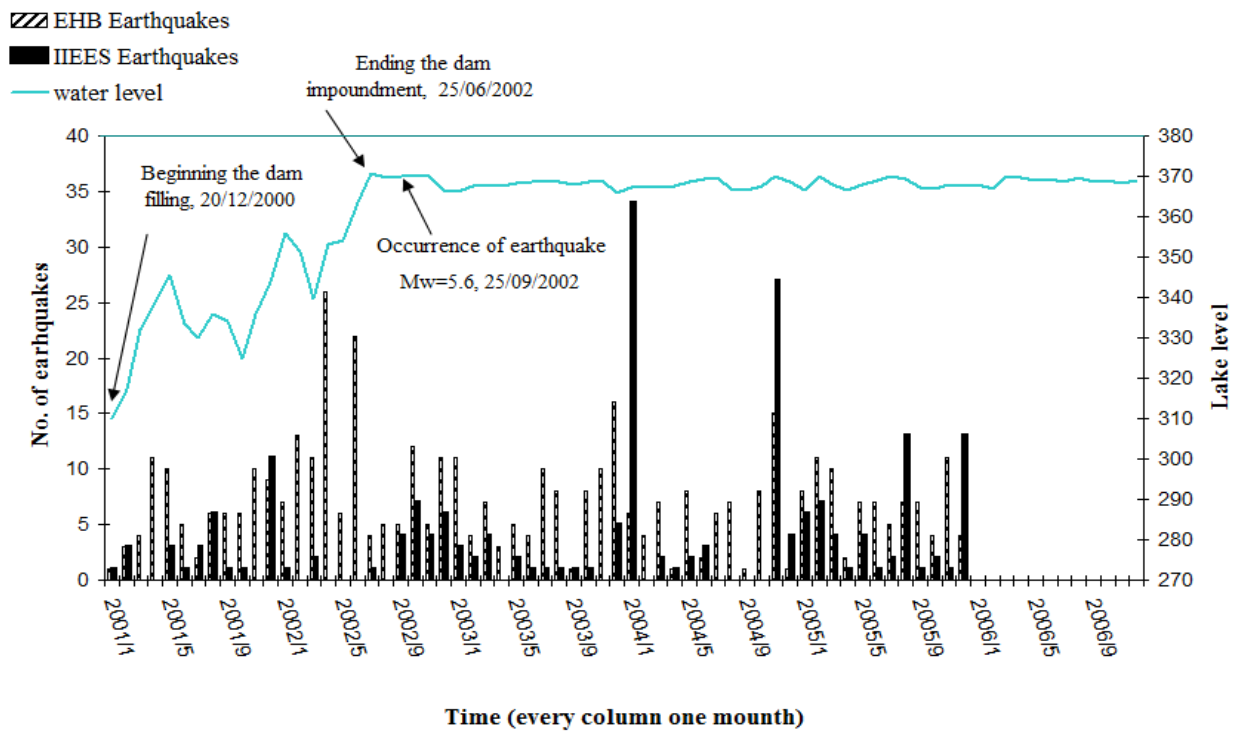


Figure 3.1. Temporal variation of initial seismicity registered by IIEES and EHB catalogs and water level changes in the Masjed Soleyman region.

As it can be seen from Fig. 3.1, after filling up the dam have started, water level increased, since then one can obviously observe the increasing rate of seismicity especially for EHB catalog. The upward trend in water level associated with rising in seismicity continued for 16 months and peaked at 370m in June 25, 2002. In September 25, 2002, ninety days after completing the impoundment, an earthquake with moment magnitude of $M_w=5.6$ had occurred in the dam area. The given epicenter by CMT for this earthquake is not reliable because of location errors, but aftershocks of this earthquake, recorded by a single station installed just after the main shock in the dam site by considering a maximum error location of ± 5 km, have been located in the south part of the dam area (see Fig. 3.2). Therefore we expect that the main shock should be in the same position as its aftershocks location.

Regards to occurring the earthquake with moment magnitude of $M_w=5.6$ in September 25, 2002 in the vicinity of dam and the relation of occurring this earthquake with the time of completing the impoundment, ninety days after finishing the impoundment, and also the increasing rate of seismicity associated with increasing rate of water level, altogether indicates that this earthquake is related to the impoundment of dam and had been induced by the loading effect of lake in the dam area.

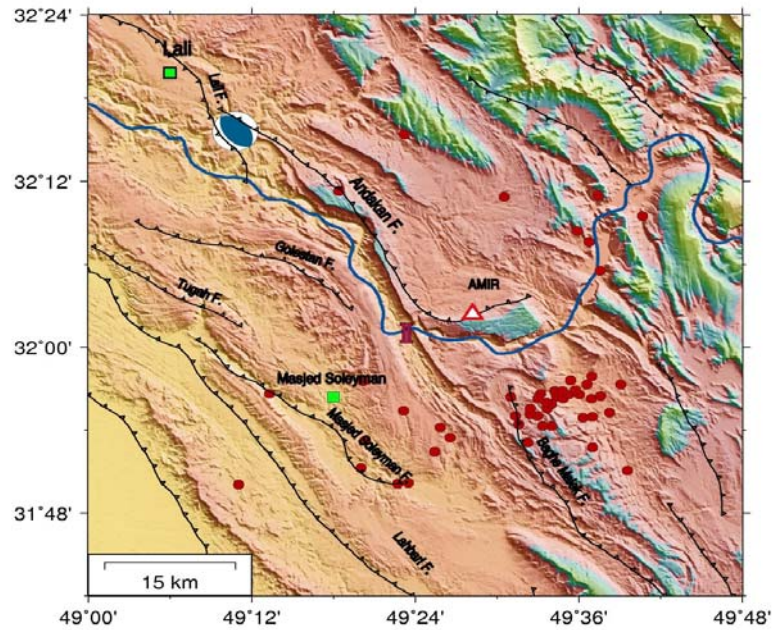


Figure 3.2. Located aftershocks of earthquake occurred in 25/09/2002 with moment magnitude of $M_w=5.6$ by a single station, location and focal mechanism of this earthquake given by CMT.

Due to installation the local seismographic network of Masjed Soleyman dam four years after completing the impoundment, in this section we try to study the relation between water level changes and seismicity in the area. We hope that regards to the data's of this network, protracted seismicity of the area could be studied.

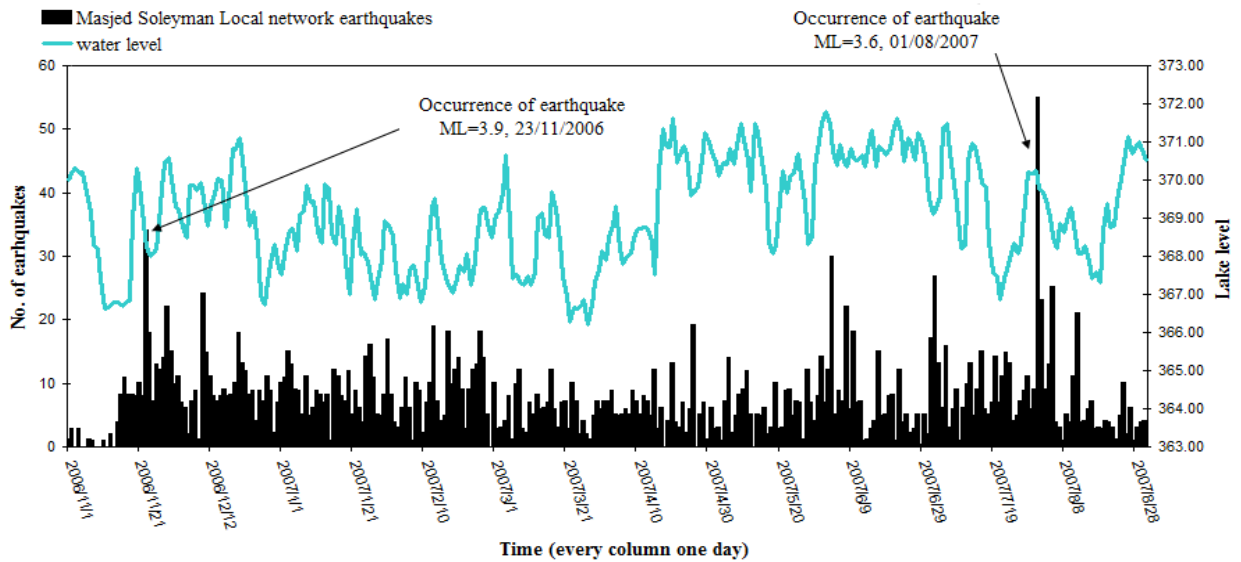


Figure 3.3. Temporal variation of protracted seismicity registered by local network installed in the dam area and water level changes in the Masjed Soleyman region.

According to Fig. 3.3, by comparing daily water level changes and seismicity, one can clearly see that increasing in seismicity is accompanied with increase in water level.

In Fig. 3.3, there are two obvious changes in seismicity of area that occurred in November 23, 2006 and August 1, 2007; both of them are accompanied with a sharp rise in water level. The greatest earthquakes registered during the monitoring the dam site has occurred in the time of occurrence of

these two rapid changes which had the magnitudes of $M_L=3.9$ and $M_L=3.6$, respectively (see Fig. 2.1). In the first case changes in water level from 368m to 371m caused 34 earthquakes in the maximum water level in one day, the greatest earthquake occurred in this day has the magnitude with $M_L=3.9$. The second case accompanied a rapid increase in water level from 367m to 370m, caused 55 earthquakes in the maximum water level in one day and the largest earthquake for this day has the local magnitude of $M_L=3.6$.

Therefore due to these observations, undoubtedly one can see the relation between the water level changes and frequency of occurrence of earthquakes in the dam area, hence protracted seismicity is continued in the dam site.

3.2. Foreshocks and Aftershocks Patterns

Gupta et al. (1972) indicated that the foreshock-aftershock patterns of reservoir induced earthquakes are similar to Mogi's type II model, whereas, the normal earthquakes belong to the type I model.

Mogi (1963) has classified the foreshock-aftershock patterns found in the experimental models into three types, as shown in Fig. 3.4, and has compared them with the natural earthquake sequences. In the type I model, structure of materials is homogeneous and external stress is uniformly distributed, and there is no foreshock activity before the main shock. In type II pattern, there is a pronounced foreshock activity prior to the main shock followed by a strong aftershock activity, in this type structure of materials is heterogeneous in some degree and distribution of external stress is not uniform. A swarm type of activity, giving Mogi's type III pattern, in this type structure of materials is extremely heterogeneous and distribution of external stress is very concentrated.

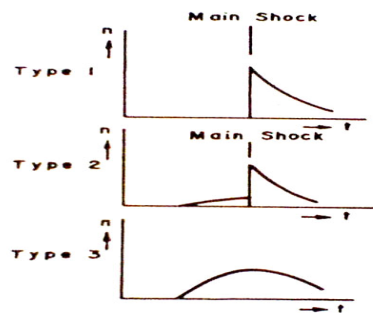


Figure 3.4. Foreshocks and aftershocks patterns for earthquakes (Mogi, 1963).

As it can be seen from Fig. 3.3, there is two abrupt changes in the frequency of earthquakes, both of them clearly show a very good coherence with Mogi's type II model which have been presented for reservoir induced earthquakes.

3.2. Correlation Between The Fractal Dimension and The b-Value

The fractal dimension (D) characterizes the degree to which the fractal fills up the surrounding space. It gives vital information about the stability of a region, and a little change in it corresponds to the dynamic evolution of the state of the system. Tosi (1998) suggested that fractal dimensions of seismicity are bound to range between 0 and 2 that is dependent on the dimension of the embedding space. A set with $D \rightarrow 0$ describes that all events clustered into one point, and $D \rightarrow 2$ infers that the events are randomly or homogeneously distributed over a two-dimensional embedding space.

In this work we try to understand the loading impact affected by impoundment of reservoir on both the parameters D and b-value, which is a unique contribution for this area.

The most commonly used method for calculation the fractal dimension of earthquake hypocenter is the correlation dimension, D_c (Grassberger & Procaccia 1983):

$$D_c = \lim_{r \rightarrow 0} \frac{\log C(r)}{\log r}, \quad (3.1)$$

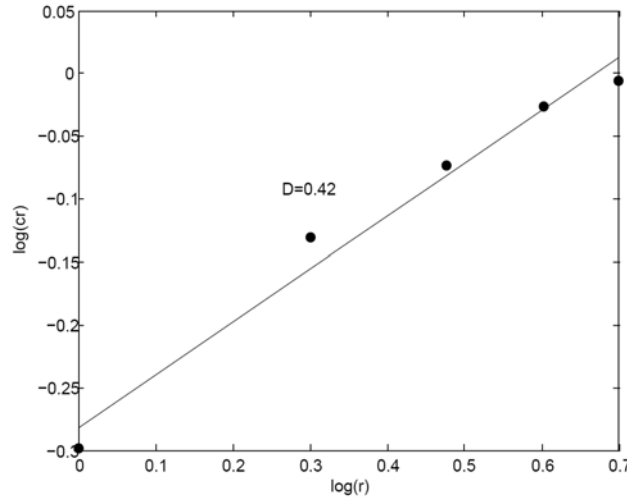


Figure 3.5. An example of estimation of D from correlation integral, log–log plot of $C(r)$ and r .

Where r is the radius of a sphere of investigation, and $C(r)$ is the correlation integral:

$$C(r) = \lim_{N \rightarrow \infty} \frac{1}{N^2} \sum_{i=1}^N \sum_{j=1}^N H(r - |x_i - x_j|), \quad (3.2)$$

Where N is the number of points in the analysis window, the x are the coordinates of the hypocenters, and H is the Heaviside step function $H(x) = 0$ for $x \leq 0$, $H(x) = 1$ for $x > 0$. In simpler terms, $C(r)$ is a function of the probability that two points will be separated by a distance less than r . fractal dimension is estimated by fitting a least-square line, the resulting plot of $\log_{10}C(r)$ against $\log_{10}(r)$ will be a straight line whose gradient corresponds to the fractal dimension (see Fig. 3.5).

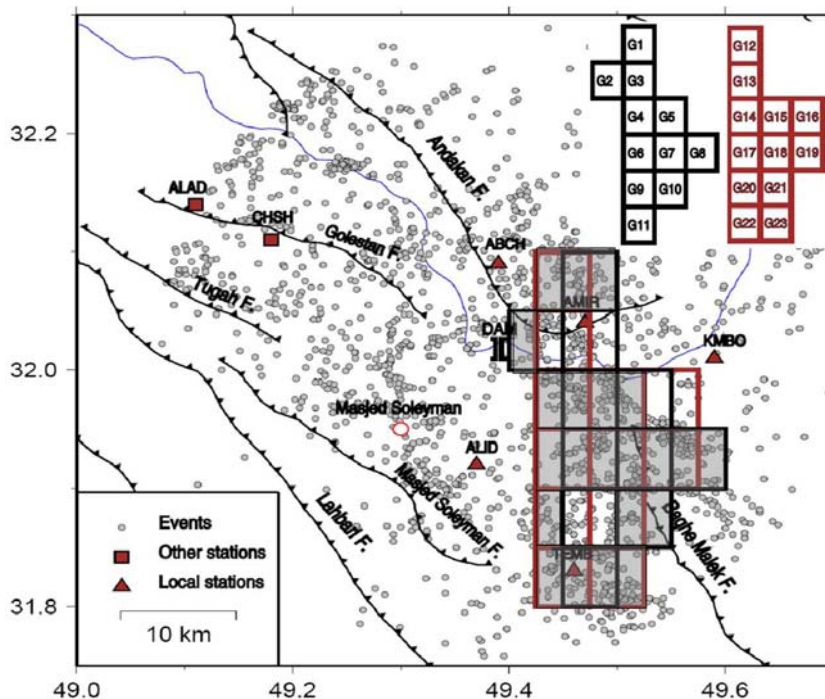


Figure 3.6. A map showing different grids considered in the study area, shaded grids enjoying b -values greater than 0.8 and D -values lower than 0.6.

To map the variation of fractal dimension as a function of space, the entire area was set into $0.05^\circ \times 0.05^\circ$ grids. An overlapping of 0.025° is made for a comprehensive picture of the map. This

attempt generated 23 grids (see Fig. 3.6). The grids were created interactively, and the regions with less than 40 events did not used in this estimation and are not shown in the Fig. 3.6. The number of events in each grid varies from 40 to 109. In this exercise, the fractal dimension value ranged from 0.40 to 0.93, but the values are less than 1 (see Fig. 3.7.a).

One of the basic seismological parameters used to describe an ensemble of earthquakes is the b-value in the frequency-magnitude relation. It characterizes the distribution of earthquakes over the observed range of magnitudes. The earthquake sizes have a power-law distribution that can be expressed in terms of the Gutenberg–Richter relation (Gutenberg and Richter, 1944). The b-value is normally 1.0, but it varies from 0.5 to 1.5 depending on the tectonic setting of a seismically active region.

The number of earthquakes N with magnitude greater than M is related to the magnitude by $\log N = a - bM$, which is widely known as the Gutenberg–Richter relation (Gutenberg & Richter 1944). In this study, the b-value of the Gutenberg–Richter relation was estimated by a maximum likelihood method.

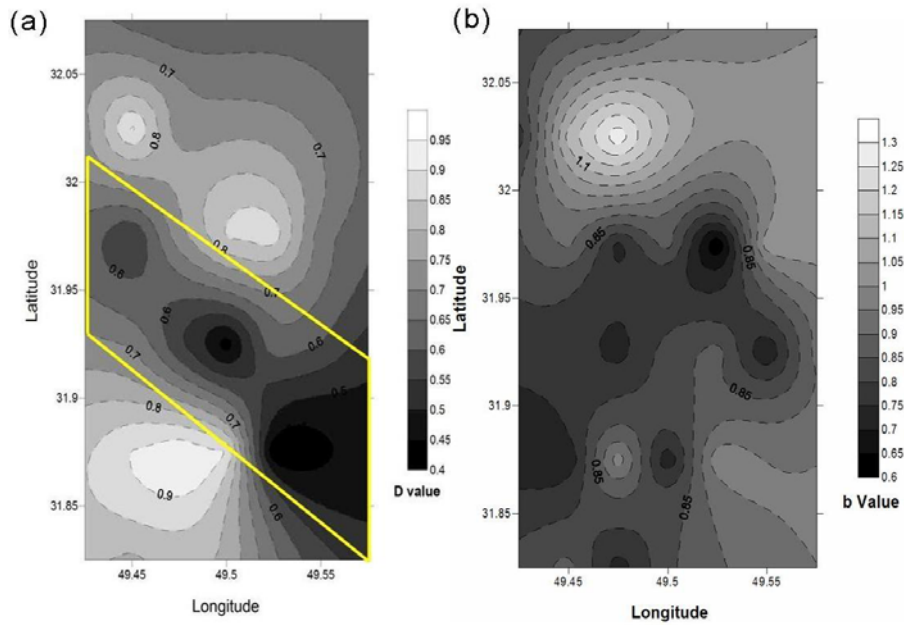


Figure 3.7. (a) Fractal dimension (D-value) contour map; (b) b-value contour map.

Maximum likelihood estimation for the b-value is claimed to be a better estimation as given by Aki (1965):

$$b = \frac{\log_{10} e}{\bar{M} - M_0} \quad (3.3)$$

Where \bar{M} is the average magnitude and M_0 is the threshold magnitude. The threshold magnitude of 0.9 has been found by examining the log-linear plot of cumulative number of events versus magnitude (see Fig. 3.8), we have obtained a b-value in the area that varies from 0.6 – 1.3 (see Fig. 3.7.b).

An estimate of error of the b-value is obtained by using the empirical formula of Pickering et al. (1995) based on a Monte Carlo simulation of the sampling effect on the exponent of a power-law distribution. The formula is as follows:

$$\sigma = b \sqrt{\frac{1}{N}} \quad b \geq 1, \quad (3.4)$$

$$\sigma = \sqrt{\frac{b}{N}} \quad b < 1, \quad (3.5)$$

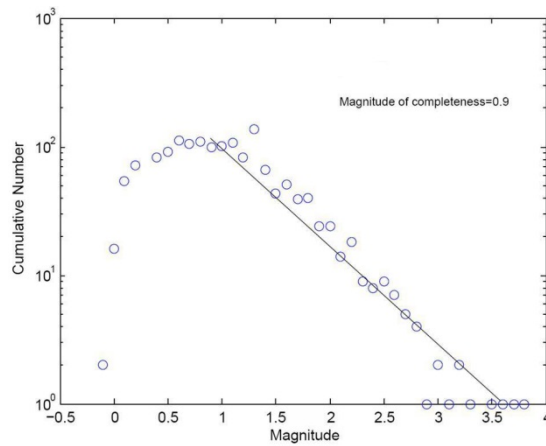


Figure 3.8. An example of estimation of b-value and M_c .

Where σ is the standard deviation of the b-value estimate and N is the sample size. Based on the Eqn. 3.4 and Eqn. 3.5 we have estimated the errors for b-value that range from ± 0.081 to ± 0.167 .

4. DISCUSSION AND CONCLUSION

The correlation between water level and seismicity of area is one of the important factors in induced earthquakes. In the Masjed Soleyman region, whenever water level increased, frequency of occurrence of earthquakes also increased and there was a positive correlation between them (see Fig. 3.1 & Fig. 3.3). The most important factors causing induced earthquakes in a large reservoir are loading effect added by the weight of reservoir and fluid pore pressure diffusion that seeps into cracks underground or along a fault.

According to Fig. 3.1, there was a distinct correlation between occurrence of earthquake with moment magnitude of $M_w=5.6$ and water level changes. Earthquakes registered by IIEES and EHB catalogs showed an increasing rate by increasing in water level, and ninety days after finishing the impoundment this earthquake occurred. Aftershocks of this earthquake have been located in the south part of the dam, near the Baghe-Malek fault (see Fig. 3.2). A very close relation between the time of occurrence, finishing the impoundment of the reservoir and increasing rate of seismicity altogether indicate that the earthquake occurred in 25/09/2002 with moment magnitude of $M_w=5.6$ in the Masjed Soleyman area is induced by the reservoir.

Comparing water level changes and seismicity of area after establishing the local network also showed a positive correlation. As it is shown in Fig. 3.3, increasing in seismicity is accompanied with increase in water level and incidence of two rapid changes in water level resulted in occurrence of two events with local magnitudes of $M_L=3.9$ and $M_L=3.6$. Therefore we can say that in Masjed Soleyman area induced seismicity is happening in both initial and protracted type.

Mogi (1962) has carried out detailed laboratory studies on foreshock-aftershock patterns and has compared them with natural earthquake occurrences. According to him, homogeneous media characterized by earthquakes with no foreshocks, slightly heterogeneous media have number of foreshocks preceding the main earthquake, and extremely heterogeneous media characterized by a swarm type of earthquake activity (see Fig. 3.4). As it can be seen from Fig. 3.3, frequencies of occurrence of two selected earthquakes are following the Mogi's type II model.

As it is shown in Fig. 3.7, we have obtained a fractal dimension (D) and b-value that varies from 0.4 to 0.93 and 0.6-1.3, respectively. The values for D -value are less than 1; the low D -value may have several explanations. Seismic activity in the Masjed Soleyman reservoir site occurs in a small area, and the distances between mainshocks and aftershocks are very small (sometimes less than 3 km) which can result in a low D -value. The seismicity of Masjed Soleyman region is due to the fault interactions and reservoir-triggered forces that generate earthquakes in small clusters. Since our data are in protracted step of seismicity in the area and the main factors for occurrence of earthquakes in this step are seepage of fluid in the crust and increase in pore pressure diffusion, therefore high

permeability and presence of fluids in the fault and surrounding area may reduce effective stresses and show relatively low Values for D, as observed by Barton et al. (1999) in Long Valley, California. The low D-value could also be seen by the effect of high pore fluid pressure in the region, as pore fluid pressure reflects redistribution of stress in the substratum. When D tends to zero, the seismicity of the area may not be due to any particular fault but may be connected to the stress generated by high pore fluid pressure; this indicates the point source zone (Tosi, 1998). Having high b-value in the studied region especially in the vicinity of dam indicates heterogeneous stress distribution in the crust whereas homogeneous stresses results in lower b-values (Mogi, 1963). Gupta et. al. (1972) showed that higher b-values in induced earthquakes are due to heterogeneous quality of distributed stress by the reservoir. Simpson (1976) showed that gradual increase in pore pressure is the main factor in the occurrence of induced earthquakes, whereas this increase could be the result of faults weakening due to pore pressure diffusion, therefore we could see a heterogeneous stress distribution in the area and high b-values.

Lower D-values ($D \leq 0.6$) and higher b-values ($b \geq 0.8$) in the major of grids except G3, G9, G13 and G16 (see Fig. 4.1) which their location is shaded in Fig. 3.6, indicates that there is a heterogeneous structure in these area and it seems that this parts are more susceptible for occurrence of induced earthquakes. Generally, for areas where induced earthquakes occur, always b-values are high while D value in these areas is low. As it said before, the key reasons for low D-values and high b-values are seepage of water in the crust and pore pressure diffusion which actually are the main reasons for the incidence of induced earthquakes. As it can be seen from Fig. 3.7.a and Fig. 2.1, the selected region which has the lower D-values is the region that dam site is located in it; therefore we could ascribe the low D-value of the region to the increasing rate of pore pressure diffusion caused by dam. It seems that earthquakes occurred in the south part of dam especially in the tag end of Baghe-Malek fault (see Fig. 2.1) are induced ones.

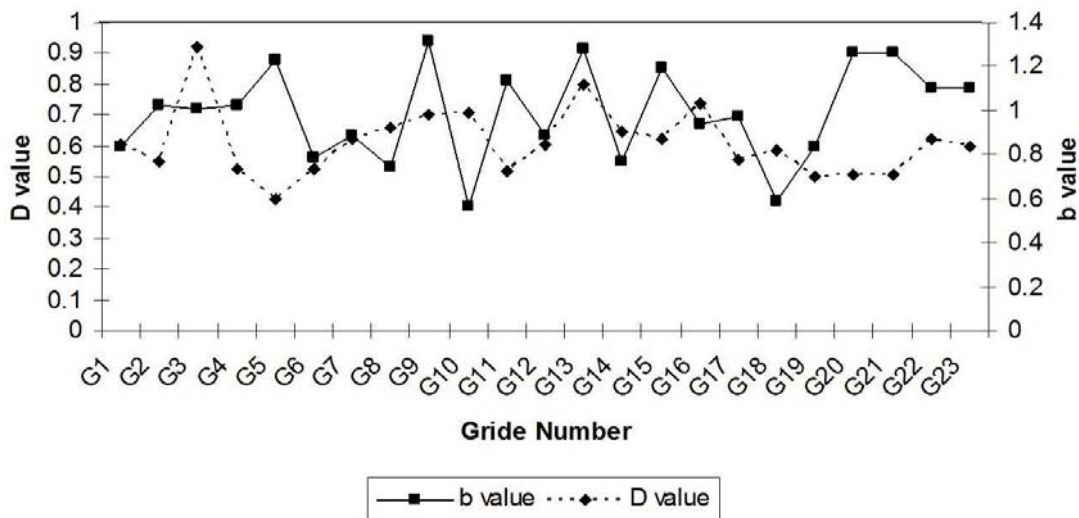


Figure 4.1. Variations of D-value and b-value within the different grids of the study area.

To conclude with, we could clearly acquire a very close compatibility showing induced seismicity from our observations, such as:

Aftershocks of the earthquake occurred in 25/09/2002 with magnitude $M_w=5.6$ are very close to the dam site (see Fig. 3.2).

Two largest earthquakes with $M_L=3.9$ and $M_L=3.6$ which registered by local network, located in the same part as of aftershocks of earthquake with $M_w=5.6$ in 25/09/2002, which all of them were near the dam site (see Fig. 2.1 and Fig. 3.2).

A very close correlation between the occurrences of earthquakes with water level changes (see Fig. 3.1 and Fig. 3.3).

Accordance of frequency of occurrence of two largest earthquakes with $M_L=3.9$ and $M_L=3.6$ which registered by local network with Mogi's type II model (see Fig. 3.3 and Fig. 3.4).

The lower values for fractal dimension and higher b-values in the area (see Fig. 3.6 and Fig. 3.7 and

Fig. 4.1).

Altogether, according to these observations, we could clearly say that the earthquake occurred in 25/09/2002 with moment magnitude of $M_w=5.6$ and major of earthquakes occurred in this area since impounding the reservoir in the south part of Masjed Soleyman dam and in the tag end of Baghe-Malek fault are induced ones. It could be said that impounding the dam caused heterogeneity in the crust and changed the stress distribution of area, especially in the dam region and in the tag end of Baghe-Malek fault, results in increasing rate of seismicity and occurrence of induced earthquakes in this region.

The 25/09/2002 Masjed Soleyman earthquake with moment magnitude of $M_w=5.6$ is truly the biggest induced earthquake that have been occurred and recognized in Iran.

ACKNOWLEDGEMENT

The authors would like to thank the managements of the International Institute of Earthquake Engineering and Seismology (IIEES) and Iran Water and Power Resources Development Company (IWPCo) for providing the opportunity and encouragement to carry out this project. We also appreciate deeply our colleagues from both the IIEES and IWPCo for their co-operation during the fieldwork.

REFERENCES

- Aki, K. (1965). Maximum likelihood estimate of b in the formula $\log N=a-bM$ and its confidence limits. *Bull. Earthquake Res. Inst. Tokyo Univ.* **43**, 237–239.
- Barton, D.J., Foulger, G.R., Henderson, J.R. and Julian, B.R. (1999). Frequency-magnitude statistics and spatial correlation dimensions of earthquakes at Long Valley Caldera, California. *Geophys. J.* **138**, 563–570.
- Grassberger, P. and Procaccia, I. (1983). Measuring the strangeness of strange attractors. *Phys. D* **9**, 189–208.
- Gupta, H.K., Rastogi, B.K. and Hari Narain (1972). Common features of the reservoir associated seismic activities. *Bull. Seis. Soc. Am.* **62:2**, 481- 492 .
- Gupta, H.K., Rastogi, B.K. (1976). Dams and earthquakes, Elsevier, Amsterdam.
- Gutenberg, B. and Richter, C.F. (1944). Frequency of earthquakes in California, *Bull. Seismol. Soc. Am.* **34**, 185–188.
- Mekkawi, M. Grasso, J.R. Schnegg, P.A. (2004). A long-lasting relaxation of seismicity at Aswan Reservoir, Egypt, 1982– 2001. *Bull. Seismol. Soc. Am.* **94:2**,479–492.
- Mogi, K. (1963). Some discussions on aftershock , foreshocks and earthquake swarms – the fracture of semi-infinite body caused by an inner stress origin and its relation to the earthquake phenomena (third paper), *Bull. Earthquake Res. Inst.* **41** , 615-658.
- Roeloffs, E.A. (1988). Fault stability changes induced beneath a reservoir with cyclic variations in water level. *J. Geophys Res* **93**,2107–2124.
- Simpson, D.W., Leith, W. and Scholtz, C.H. (1988). Two types of reservoir-induced seismicity. *Bull. Seismol. Soc. Am.* **75**, 2025–2040.
- Snow, D.T. (1972). Geodynamics of seismic reservoirs. In Proceedings of the Percolation through Fissured Rocks, T2-J, Stuttgart, *Ges. Erd. Grundbau*, 1–19.
- Tosi, P. (1998). Seismogenic structure behaviour revealed by spatial clustering of seismicity in the Umbria-Marche Region (central Italy), *Ann. Geophys.* **41**, 215–224.